Acta Mechanica Solida Sinica, Vol. 25, No. 4, August, 2012 ISSN 0894-9166
Published by AMSS Press, Wuhan, China

SINGLE AND DOUBLE EDGE INTERFACE CRACK SOLUTIONS FOR ARBITRARY FORMS OF MATERIAL COMBINATION

Xin Lan⋆ **Nao-Aki Noda** **Yu Zhang** **Kengo Michinaka**

(*Department of Mechanical Engineering, Kyushu Institute of Technology, Japan*)

Received 19 October 2011

ABSTRACT In this paper interfacial edge crack problems are considered by the application of the finite element method. The stress intensity factors are accurately determined from the ratio of crack-tip-stress value between the target given unknown and reference problems. The reference problem is chosen to produce the singular stress fields proportional to those of the given unknown problem. Here the original proportional method is improved through utilizing very refined meshes and post-processing technique of linear extrapolation. The results for a double-edge interface crack in a bonded strip are newly obtained and compared with those of a single-edge interface crack for different forms of combination of material. It is found that the stress intensity factors should be compared in the three different zones of relative crack lengths. Different from the case of a cracked homogeneous strip, the results for the double edge interface cracks are found to possibly be bigger than those for a single edge interface crack under the same relative crack length.

KEY WORDS stress intensity factor, single edge interface crack, double edge interface crack, combination of material, bonded strip

I. INTRODUCTION

Composite materials and bonded structures are widely employed in the modern industrial context. The mechanical behavior of the bi-material interface is of great significance for industrial application. Since the presence of cracks affects a structure's performance and may result in damage, basic studies about the interface cracks have secured considerable attention. High stress concentration at the bonding edge corner caused by differences in the elastic properties of its material components may lead to the initiation of micro-cracks and then propagation. Therefore, the single and double edge interface cracks will be mainly investigated in this research.

Asymptotic solutions to the singular stress field near the interface corner have not been found until recently[1–9]. However, multiple/oscillatory singularity adds to the difficulty in determining the stress intensity factors of the interfacial cracks. It was only shortly before that various numerical methods have been reported to determine the stress intensity factors of an interface crack. Specifically, Wu[10] suggested calculating the stress intensity factors at the tip of an interface crack based on an evaluation of the J-integral by the virtual crack extension method. Yang and Kuang[11] established a path independent contour integral method for the stress intensity factors of the interface crack. Munz and Yang[12] used the FE-method to analyze the stress singularities at the interface for a rectangular bi-material bonded plate subjected to two loading conditions. Dong et al.[13] proposed procedures for stress intensity factor

⋆ Corresponding author. E-mail: xinlan_al@yahoo.com

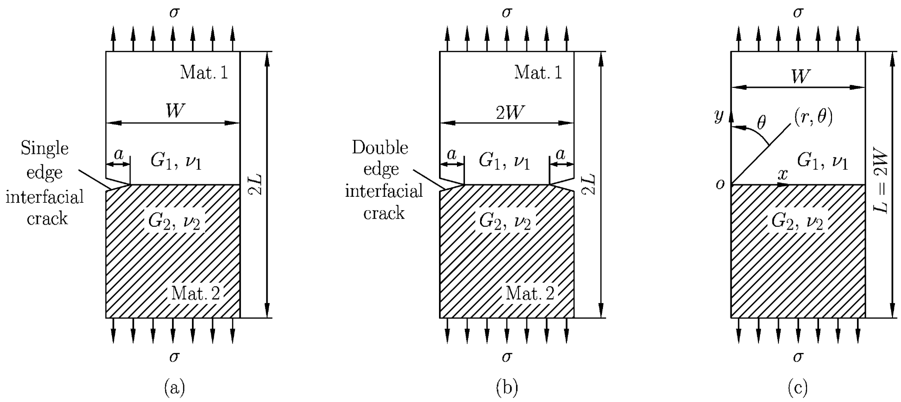

Fig. 1. (a) Single edge interface crack, (b) double edge interface crack in a bonded strip and (c) bi-material bonded strip without crack.

computation using traction singular quarter-point boundary elements. Liu et al.[14] developed a simple and effective numerical method to calculate the stress intensity factors for an interface crack with one or two singularities. Oda et al.[15] extended the crack tip method[16] to solving the interface crack problems by using the ratio of crack-tip-stress value between the given unknown and reference problems. Here, the reference problem is chosen to produce the singular stress fields proportional to the ones of given unknown problems.

In the authors' previous research, Noda et al. investigated the stress intensity factors of an edge interface crack in a bonded dissimilar semi-infinite plane[17]. Then Lan et al. discussed the effect of the material combination and the relative crack lengths of the stress intensity factors of a single edge cracked bonded strip[18]. As a further research on the authors' previous work, the study object is extended to the double edge interface crack of a bonded strip. In this paper the stress intensity factors for a bi-material bonded strip with single and double edge interface cracks as shown in Figs.1(a) and (b) will be examined using the improved proportional method. The stress intensity factors will be computed and listed by varying different forms of combination of materials and relative crack lengths. Then the values for the two different types of cracks will be compared for the whole range of combination of materials ($0 \le \alpha \le 0.95, -0.2 \le \beta \le 0.45$) and relative crack lengths ($0 \le a/W \le 0.9$). The effect of the relative crack lengths and material mismatch parameters are of special interest in this paper. It will be shown that the stress intensity factors of a double edge interface crack may be possibly larger than those of a single edge interface crack for some specific combination of materials and relative crack lengths different from the case of a cracked homogeneous strip.

II. THE ANALYTIC METHOD

2.1. Physical Background

Recently, an effective method has been proposed for computing the stress intensity factors in a cracked homogeneous plate[16]. Then, the method was successfully extended to the interfacial crack problems[15]. Both methods utilize the stress component values at the crack tip computed by the FEM. For a given bi-material bonded structure, the stress intensity factors are defined as shown in Eq.(1)[19]:

$$\sigma_y + \mathrm{i}\tau_{xy} = \frac{K_{\mathrm{I}} + \mathrm{i}K_{\mathrm{II}}}{\sqrt{2\pi r}} \left(\frac{r}{2a}\right)^{\mathrm{i}\varepsilon}, \quad r \to 0 \tag{1}$$

where, σ_y, τ_{xy} denote the stress components near the crack tip. r is the radial distance from the crack tip, and ε is the bi-elastic constant given by

$$\varepsilon = \frac{1}{2\pi} \ln \frac{\kappa_1/G_1 + 1/G_2}{\kappa_2/G_2 + 1/G_1} \tag{2}$$

$$\kappa_m = \begin{cases} 3 - 4\nu_m & \text{(plane strain)} \\ \dfrac{3 - \nu_m}{1 + \nu_m} & \text{(plane stress)} \end{cases} \quad (m = 1, 2) \tag{3}$$

where G_m $(m=1,2)$ and ν_m $(m=1,2)$ are the shear moduli and Poisson's ratios of either material, respectively. The real and imaginary parts of the oscillatory stress intensity factors $K_{\rm I}+{\rm i}K_{\rm II}$ in Eq.(1) can be separated as

$$K_{\rm I}=\lim_{r\to0}\sqrt{2\pi r}\sigma_y\left(\cos Q+\frac{\tau_{xy}}{\sigma_y}\sin Q\right) \tag{4}$$

$$K_{\rm II}=\lim_{r\to0}\sqrt{2\pi r}\tau_{xy}\left(\cos Q-\frac{\sigma_y}{\tau_{xy}}\sin Q\right) \tag{5}$$

$$Q=\varepsilon\ln\left(\frac{r}{2a}\right) \tag{6}$$

For the two interface crack problems C and D shown in Figs.2(a) and (b), suppose they have the same crack lengths (half length) $a=a_0$ and the same combination of materials $\varepsilon=\varepsilon_0$. Examining the points along the interface with the same radial distances $r=r_0$ for the two problems C and D, gives $[Q^*]_{\rm C}=[Q]_{\rm D}=\varepsilon_0\ln\left(\frac{r_0}{2a_0}\right)$. By recalling Eqs.(4) and (5), a proportional relationship given in Eq.(7) is established if and only if Eq.(8) can be satisfied,

$$\frac{[K_{\rm I}]_{\rm D}}{[K_{\rm I}^*]_{\rm C}}=\frac{[\sigma_y]_{\rm D}}{[\sigma_y^*]_{\rm C}}=\frac{[\sigma_{y0,{\rm FEM}}]_{\rm D}}{\left[\sigma_{y0,{\rm FEM}}^*\right]_{\rm C}},\quad \frac{[K_{\rm II}]_{\rm D}}{[K_{\rm II}^*]_{\rm C}}=\frac{[\tau_{xy}]_{\rm D}}{[\tau_{xy}^*]_{\rm C}}=\frac{[\tau_{xy0,{\rm FEM}}]_{\rm D}}{\left[\tau_{xy0,{\rm FEM}}^*\right]_{\rm C}} \tag{7}$$

$$\left[\frac{\tau_{xy}^*}{\sigma_y^*}\right]_{\rm C}=\left[\frac{\tau_{xy}}{\sigma_y}\right]_{\rm D},\quad \left[\frac{\tau_{xy0,{\rm FEM}}^*}{\sigma_{y0,{\rm FEM}}^*}\right]_{\rm C}=\left[\frac{\tau_{xy0,{\rm FEM}}}{\sigma_{y0,{\rm FEM}}}\right]_{\rm D} \tag{8}$$

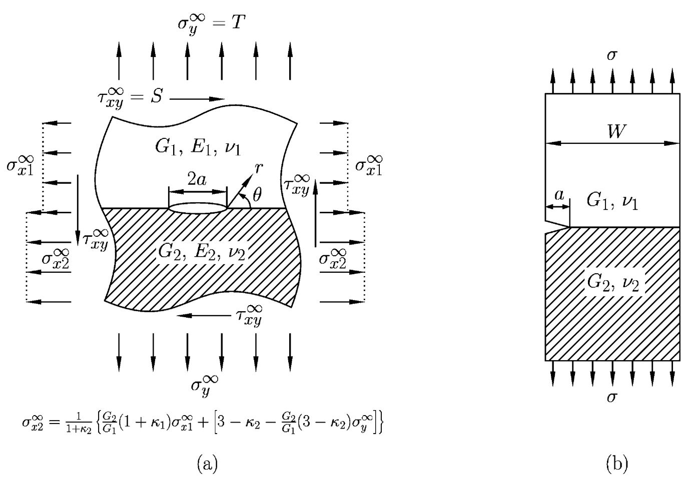

Fig. 2. Demonstration of (a) the reference problem (problem C) and (b) a given unknown problem (problem D).

Assume the stress intensity factors of problem C are given in advance and denote problem C as the reference problem, those of problem D are unknown and left to be solved (the target unknown problem). Rearranging Eq.(7) gives the stress intensity factors of the target unknown problem (problem D) as

$$[K_{\rm I}]_{\rm D}=\frac{[\sigma_{y0,{\rm FEM}}]_{\rm D}\,[K_{\rm I}^*]_{\rm C}}{\left[\sigma_{y0,{\rm FEM}}^*\right]_{\rm C}},\quad [K_{\rm II}]_{\rm D}=\frac{[\tau_{xy0,{\rm FEM}}]_{\rm D}\,[K_{\rm II}^*]_{\rm C}}{\left[\tau_{xy0,{\rm FEM}}^*\right]_{\rm C}} \tag{9}$$

Here, $\sigma_{y0,{\rm FEM}}^*$, $\tau_{xy0,{\rm FEM}}^*$ and $\sigma_{y0,{\rm FEM}}$, $\tau_{xy0,{\rm FEM}}$ are the stress components at the crack tip computed by FEM of the reference and target unknown problems, respectively.

2.2. Determination of the Reference Problems

In this study, a central cracked bonded dissimilar half-plane subjected to remote uniform tension $\sigma_y^\infty = T$ and $\tau_{xy}^\infty = S$ as shown in Fig.2(a) is treated as the reference problem. And its stress intensity factors are given by the theoretical solution as

$$K_{\mathrm{I}}^* + \mathrm{i}K_{\mathrm{II}}^* = (\sigma_y^\infty + \mathrm{i}\tau_{xy}^\infty)\sqrt{\pi a}(1+2\mathrm{i}\varepsilon), \quad \sigma_y^\infty = T, \quad \tau_{xy}^\infty = S \tag{10}$$

Let $\sigma_{y0,\mathrm{FEM}}^{*T=1,S=0}$, $\tau_{xy0,\mathrm{FEM}}^{*T=1,S=0}$ and $\sigma_{y0,\mathrm{FEM}}^{*T=0,S=1}$, $\tau_{xy0,\mathrm{FEM}}^{*T=0,S=1}$ denote the stress components of the bonded dissimilar half-plane shown in Fig.2(a) subjected to pure remote tension $(T,S)=(1,0)$ and pure remote shear $(T,S)=(0,1)$, respectively. Then, using the principle of superposition, the stress components of the reference problem shown in Fig.2(a) take the following forms:

$$\sigma_{y0,\mathrm{FEM}}^* = \sigma_{y0,\mathrm{FEM}}^{*T=1,S=0} \times T + \sigma_{y0,\mathrm{FEM}}^{*T=0,S=1} \times S \tag{11}$$

$$\tau_{xy0,\mathrm{FEM}}^* = \tau_{xy0,\mathrm{FEM}}^{*T=1,S=0} \times T + \tau_{xy0,\mathrm{FEM}}^{*T=0,S=1} \times S \tag{12}$$

As aforementioned, the condition given in Eq.(8) should be satisfied. Inserting Eqs.(11) and (12) into Eq.(8) gives the solution of S/T for determining the remote external loads applied to the reference problem.

$$\frac{S}{T} = \frac{[\sigma_{y0,\mathrm{FEM}}]_{\mathrm{D}} \times \left[\tau_{xy0,\mathrm{FEM}}^{*T=1,S=0}\right]_{\mathrm{C}} - [\tau_{xy0,\mathrm{FEM}}]_{\mathrm{D}} \times \left[\sigma_{y0,\mathrm{FEM}}^{*T=1,S=0}\right]_{\mathrm{C}}}{[\tau_{xy0,\mathrm{FEM}}]_{\mathrm{D}} \times \left[\sigma_{y0,\mathrm{FEM}}^{*T=0,S=1}\right]_{\mathrm{C}} - [\sigma_{y0,\mathrm{FEM}}]_{\mathrm{D}} \times \left[\tau_{xy0,\mathrm{FEM}}^{*T=0,S=1}\right]_{\mathrm{C}}} \tag{13}$$

When the external load for the reference problem (problem C) $\sigma_y^\infty = T$ and $\tau_{xy}^\infty = S$ can satisfy Eq.(13), Eq.(9) can be satisfied. Specifically, let $T=1$ so that S can be determined. Inserting $T=1, S$ into Eq.(10) gives the exact values of the oscillatory stress intensity factors for the reference problem (problem C). Finally, the stress intensity factors for the target unknown problem (problem D) can be yielded using the proportional relationship as given in Eq.(9). Furthermore, the oscillatory terms in the above discussion will vanish when the two materials are identical, so the current method is also applicable to cracked homogeneous plate problems.

III. NUMERICAL RESULTS AND DISCUSSION

3.1. Formulation of Single and Double Edge Interface Crack Problems for Arbitrary Combination of Materials

Regarding the bonded strip of width W and length L shown in Fig.1, the length L of the strip is assumed to be much greater than the width W ($L \geq 2W$). It is composed of two elastic, isotropic and homogeneous strips that are perfectly bonded along the interface. And the strip is subjected to a remote uniform tensile stress σ. The material above the interface is termed material 1, and the material below is termed material 2. Consider the bi-material bonded plate shown in Fig.1(c). It is assumed that a single edge crack shown in Fig.1(a) and a double one shown in Fig.1(b) with a crack length of a have initiated at the free edge corner of the bonded plate.

The stress intensity factors for the aforementioned problems in plane strain or plane stress are only determined on the two elastic mismatch parameters α and β (also known as *Dundurs' material composite parameters*, Dundurs, 1969). And the Dundurs' material composite parameters are defined as

$$\alpha = \frac{G_1(\kappa_2+1) - G_2(\kappa_1+1)}{G_1(\kappa_2+1) + G_2(\kappa_1+1)}, \quad \beta = \frac{G_1(\kappa_2-1) - G_2(\kappa_1-1)}{G_1(\kappa_2+1) + G_2(\kappa_1+1)} \tag{14}$$

where, the subscripts denote material 1 or 2, $G_m = E_m/[2(1+\nu_m)]$ $(m=1,2)$, G_m, E_m and ν_m denote shear modulus, Young's modulus and Poisson's ratio for material m, respectively. $\kappa_m = (3-\nu_m)/(1+\nu_m)$ for plane stress and $\kappa_m = (3-4\nu_m)$ for plane strain. The parameter α is positive when material 2 is more compliant than material 1, and is negative when material 2 is stiffer than material 1. In this research, only the stress intensity factors for $\beta \geq 0$ in α-β space shown in Fig.3 have been investigated since switching materials 1 and 2 (mat1 $\Leftrightarrow$ mat2) will only reverse the signs of α and β $((\alpha,\beta) \Leftrightarrow (-\alpha,-\beta))$. Furthermore, in order to facilitate discussion, all the stress intensity factors are normalized using the following equations:

$$F_{\mathrm{I}} = \frac{K_{\mathrm{I}}}{\sigma\sqrt{\pi a}}, \quad F_{\mathrm{II}} = \frac{K_{\mathrm{II}}}{\sigma\sqrt{\pi a}} \tag{15}$$

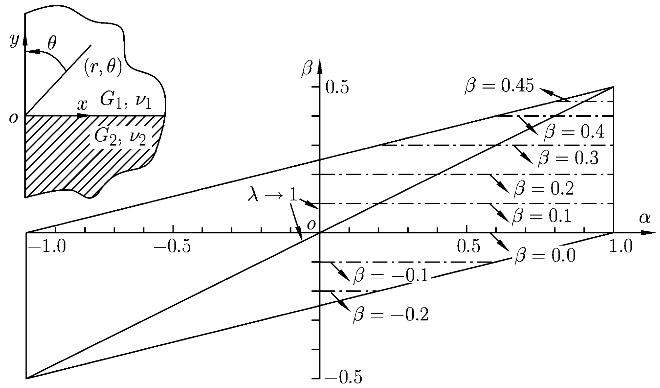

Fig. 3. α-β space for material composite parameters.

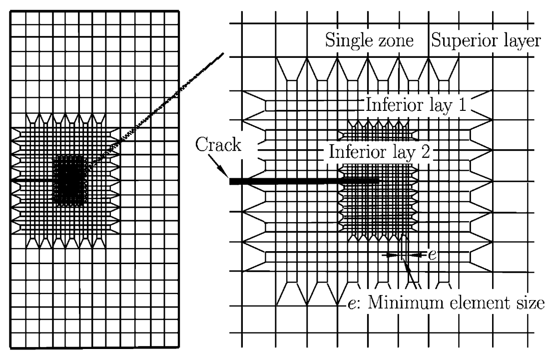

Fig. 4. FE mesh demonstration of the geometry of a single edge cracked strip (the target unknown problem).

3.2. Numerical Verification for the Single and Double Edge Crack Problems

The robustness and accuracy of the current method in treating the single and double edge cracked problems are investigated. MSC.MARC 2007 r1 finite element analysis package is used in this research. Four-node quadrilateral elements are employed to mesh the reference and the target unknown problems. Figure 4 shows the FE mesh type for a single-edge cracked homogeneous strip (target unknown problem). As can be seen from this figure, the meshes in the vicinity of the singular zone are subdivided in a self-similar manner. And the element size for each inferior layer is one-third of that of the superior one.

The stress intensity factors for the extremely deep crack cases ($a/W = 0.8$) of a single and a double edge cracked homogeneous strips are plotted against the minimum element size of the FE model in

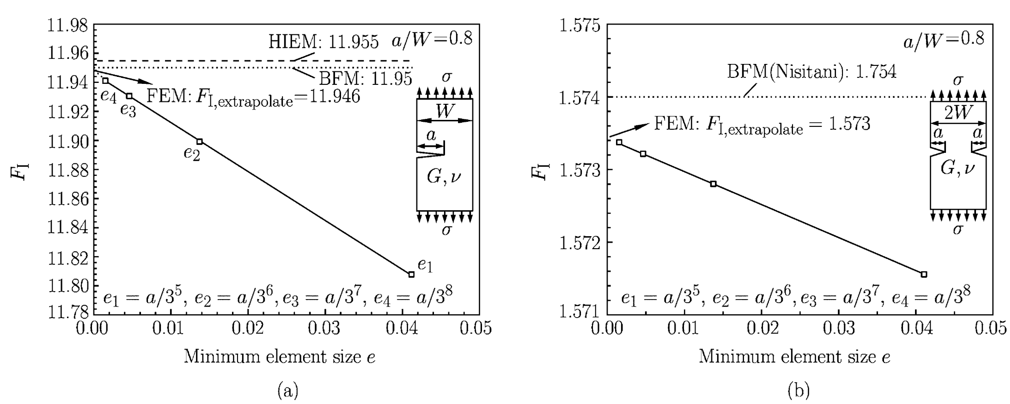

Fig. 5. Variations of the normalized stress intensity factors $F_{\mathrm{I}} = K_{\mathrm{I}}/(\sigma\sqrt{\pi a})$ with minimum element size of the FE model for the (a) single and (b) double edge cracked bonded strips.

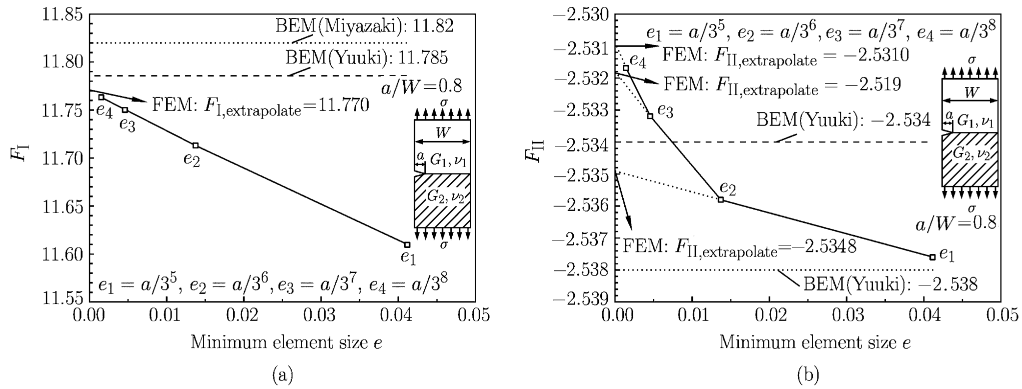

Fig. 6. Variations of the normalized stress intensity factors. (a) $F_{\mathrm{I}} = K_{\mathrm{I}}/(\sigma\sqrt{\pi a})$ and (b) $F_{\mathrm{II}} = K_{\mathrm{II}}/(\sigma\sqrt{\pi a})$ with minimum element size e for a bonded strip $a/W = 0.8$ subjected to uniform tension.

Figs.5(a) and (b), respectively. As can be seen from the figures, accurate results can be obtained using linear extrapolation. The values for other relative crack lengths of the two types of cracks are tabulated and compared with those predicted by Kaya[20], Noda[21] and Nisitani[22] in Table 1, respectively. It can be seen from the table that the extrapolated results in this research and those of Kaya[20], Noda[21] and Nisitani[22] are in very good agreement.

Table 1. **Normalized stress intensity factors $K_{\mathrm{I}}/(\sigma\sqrt{\pi a})$ for the single and double edge cracked homogeneous strips**

a/W	Single edge crack			Double edge crack	
	Present	Ref.[20]	Ref.[21]	Present	Ref.[22]
0.1	1.189	1.1892	1.189	1.117	1.117
0.2	1.367	1.3673	1.367	1.112	1.112
0.3	1.659	1.6599	1.659	1.115	1.115
0.4	2.111	2.1114	2.111	1.132	1.132
0.5	2.824	2.8246	2.823	1.169	1.169
0.6	4.031	4.0332	4.032	1.236	1.236
0.7	6.352	6.3549	6.355	1.353	1.353
0.8	11.946	11.955	11.95	1.573	1.574
0.9	34.593	34.633	34.62	2.115	2.116

Table 2. **Normalized stress intensity factors for a single edge cracked bonded strip shown in Fig.1(a)** ($G_2/G_1 = 4$, $\nu_1 = \nu_2 = 0.3$, **plane stress)**

a/W	$F_{\mathrm{I}} = K_{\mathrm{I}}/(\sigma\sqrt{\pi a})$				$F_{\mathrm{II}} = K_{\mathrm{II}}/(\sigma\sqrt{\pi a})$			
	Present	Ref.[23]	Ref.[24]	Ref.[25]	Present	Ref.[23]	Ref.[24]	Ref.[25]
0.1	1.209	1.199	1.201	1.209	−0.2393	−0.237	−0.238	−0.239
0.2	1.368	1.368	1.387	1.368	−0.250	−0.251	−0.254	−0.250
0.3	1.653	1.655	1.653	1.654	−0.288	−0.288	−0.288	−0.288
0.4	2.100	2.102	2.100	2.101	−0.359	−0.358	−0.359	−0.359
0.5	2.805	2.806	2.807	2.807	−0.484	−0.483	−0.483	−0.483
0.6	3.998	4.001	4.000	4.006	−0.716	−0.714	−0.716	−0.716
0.7	6.285	6.298	6.298	6.304	−1.207	−1.204	−1.209	−1.208
0.8	11.770	11.780	11.785	11.82	−2.532	−2.515	−2.534	−2.538

Figures 6(a) and (b) show the variation of the normalized stress intensity factors $F_{\mathrm{I}} = K_{\mathrm{I}}/(\sigma\sqrt{\pi a})$ and $F_{\mathrm{II}} = K_{\mathrm{II}}/(\sigma\sqrt{\pi a})$ for a single edge cracked dissimilar bonded strip $a/W = 0.8$. The elastic parameters are restricted to $G_2/G_1 = 4$, $\nu_2 = \nu_1 = 0.3$ and plane stress condition is assumed in the analysis. As can be seen from Fig.6(a), a linear relationship can be observed for the case of $K_{\mathrm{I}}/(\sigma\sqrt{\pi a})$. However,

Table 3. **Normalized stress intensity factors for a double edge cracked bonded strip shown in Fig.1(b) ($\nu_1 = \nu_2 = 0.3$, plane stress)**

a/W	$E_2/E_1 = 2$		$E_2/E_1 = 4$		$E_2/E_1 = 10$		$E_2/E_1 = 100$	
	$K_{\rm I}/(\sigma\sqrt{\pi a})$	$K_{\rm II}/(\sigma\sqrt{\pi a})$	$K_{\rm I}/(\sigma\sqrt{\pi a})$	$K_{\rm II}/(\sigma\sqrt{\pi a})$	$K_{\rm I}/(\sigma\sqrt{\pi a})$	$K_{\rm II}/(\sigma\sqrt{\pi a})$	$K_{\rm I}/(\sigma\sqrt{\pi a})$	$K_{\rm II}/(\sigma\sqrt{\pi a})$
0.1	1.131	−0.128	1.164	−0.241	1.212	−0.350	1.264	−0.447
0.2	1.115	−0.119	1.122	−0.219	1.132	−0.309	1.142	−0.382
0.3	1.115	−0.112	1.113	−0.204	1.112	−0.284	1.1109	−0.347
0.4	1.131	−0.106	1.128	−0.193	1.124	−0.268	1.120	−0.325
0.5	1.168	−0.103	1.166	−0.188	1.163	−0.259	1.159	−0.315
0.6	1.236	−0.104	1.235	−0.189	1.235	−0.261	1.234	−0.318
0.7	1.354	−0.111	1.356	−0.202	1.358	−0.280	1.361	−0.342
0.8	1.575	−0.133	1.580	−0.243	1.586	−0.338	1.591	−0.414
0.9	2.118	−0.207	2.122	−0.380	2.128	−0.531	2.133	−0.652

no simple linear behavior is observed for the case of $K_{\rm II}/(\sigma\sqrt{\pi a})$ in Fig.6(b). It should be noted that a post-processing technique of linear extrapolation is used to compute both the values of $F_{\rm I} = K_{\rm I}/(\sigma\sqrt{\pi a})$ and $F_{\rm II} = K_{\rm II}/(\sigma\sqrt{\pi a})$ in this research. The extrapolated values of other relative crack lengths are tabulated in Table 2 together with those of Matsumto[23], Yuuki[24] and Ikeda[25]. Table 2 illustrates that the stress intensity factor values computed by the current method are in very good agreement with those predicted by Matsumto[23] , Yuuki[24] and Ikeda[25]. And the worst computational errors relative to those of Ikeda are error$(K_{\rm I}/(\sigma\sqrt{\pi a})) = 0.13\%$ and error$(K_{\rm II}/(\sigma\sqrt{\pi a})) = 0.03\%$ for the deep edge crack case $a/W = 0.8$.

The stress intensity factors for a double edge cracked bonded strip shown in Fig.1(b) are tabulated in Table 3. Linear extrapolation is also employed for this case. The results in Table 3 are new and with no published data to be compared with them. As shown in the previous examples, the current method is found to produce accurate numerical values for mode I cracks; and therefore, Table 3 is also reliable.

3.3. Stress Intensity Factors for the Single and Double Edge Interface Cracks in a Bonded Strip

In this section, the stress intensity factors at the crack tip for a double edge interface crack in a bi-material bonded strip are systematically investigated for various material combinations and crack lengths. For the case of a single and a double edge cracked homogeneous strips shown in Fig.7, it is well known that the stress intensity factors of the single crack are always no smaller than those of the double crack. However, this law should not be always true of the case of interfacial cracks. The stress intensity factors for the single and double edge interface cracks will be compared for arbitrary combinations of materials in the following section.

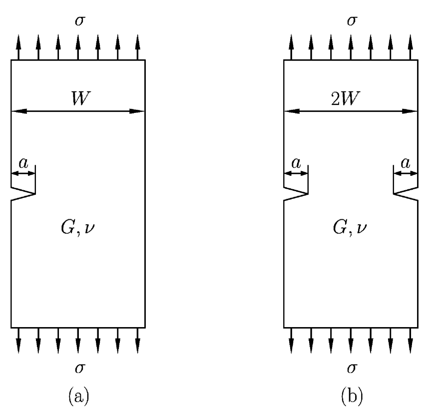

Fig. 7. (a) Single and (b) double edge cracks in homogeneous strips.

3.3.1. Stress intensity factors for the double edge interface cracks within the zone of free-edge singularity

In the authors' previous research, it has been confirmed that the normalized stress intensity factors within the zone of free-edge singularity for a single edge cracked bonded strip exhibit a linear double logarithmic relationship with the relative crack length a/W[17]. Here, what is of interest is mainly the double edge interface cracks. The stress intensity factors will be investigated by varying the relative crack length a/W, as well as the material composite parameters α and β. Then the stress intensity factors for those two interfacial cracks will be compared systematically. We restrict our discussion to the material combinations with $\beta = 0.3$, and the same phenomenon can be found from other forms of combination of material. The double logarithmic distributions of the normalized stress intensity factors F_{I} and F_{II} for the single and double edge interface cracks are plotted against a/W as shown in Figs.8(a) and (b), respectively. The values of F_{I}, F_{II} for the double edge interface cracks are plotted in solid curves and those for the single edge interface cracks are plotted in dashed ones. From Fig.8, it can be found that, similar to the case of the single edge interface crack, the double logarithmic distributions of F_{I}, F_{II} for a double-edge cracked bonded strip also exhibit linearity when $a/W < 0.01$. Furthermore, the slopes corresponding to the same material composite parameters for the two crack cases are totally identical, and they are equal to the singular index $\lambda - 1$ of the perfectly bonded strip without a crack as shown in Fig.1(c). This proves that the singular zone for a shallow edge interface crack is controlled by the stress state near the interface corner of the corresponding un-cracked bonded strip. Recently the singular field at the interface corner for a bonded strip as shown in Fig.9(a) has been studied in several publications[1–9]. If an interface crack is introduced as shown in Fig.9(b), the stress intensity factors are controlled by the stress states near the corner in which the free edge intersects the interface.

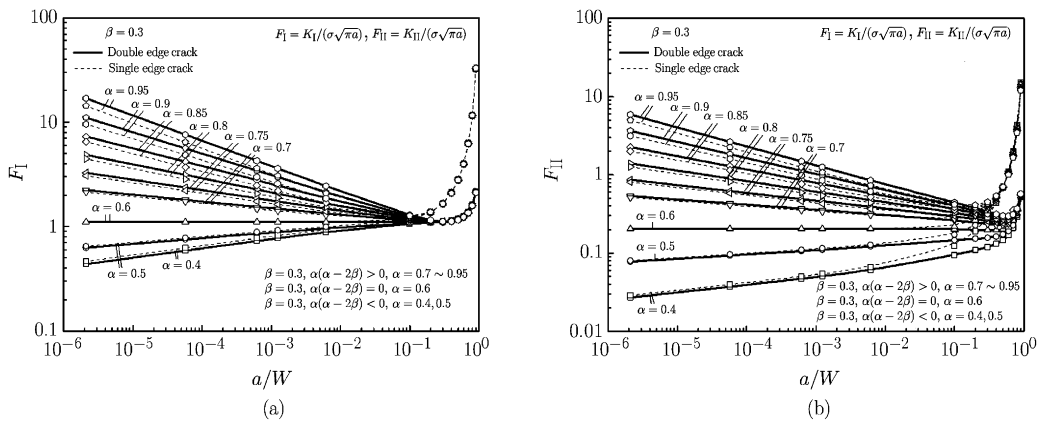

Fig. 8. Double logarithmic distributions of (a) $F_{\mathrm{I}} = K_{\mathrm{I}}/(\sigma\sqrt{\pi a})$ and (b) $F_{\mathrm{II}} = K_{\mathrm{II}}/(\sigma\sqrt{\pi a})$ for the single and double edge interface cracks.

The double logarithmic discussion about the case of a single edge interface crack in Ref.[17] is also applicable to the case of a double edge interface crack. An empirical function as Eq.(16) was proposed to compute $F_{\mathrm{I}}, F_{\mathrm{II}}$ of a single edge interface crack within the singular zone of a bonded strip[17]. Where F_{I}, F_{II} are the normalized stress intensity factors, a/W is the relative crack length, $1 - \lambda$ is the order of stress singularity for the perfectly bonded strip without crack and C_{I}, C_{II} are constants determined by the material composite parameters and crack type. It has been proved that Eq.(16) is also suitable for the double edge crack case by modifying the constants C_{I}, C_{II}. Here, what should be noticed is that F_{I}, F_{II} are the same within the singular zone for the two types of cracks when $\alpha\,(\alpha - 2\beta) = 0$ (see, the curve of $\alpha = 0.6$, $\beta = 0.3$, $a/W < 0.01$ in Fig.8). Detailed information can be found in Ref.[17].

$$F_{\mathrm{I}} \cdot (a/W)^{1-\lambda} = C_{\mathrm{I}}, \quad F_{\mathrm{II}} \cdot (a/W)^{1-\lambda} = C_{\mathrm{II}} \tag{16}$$

For the bonded strip without crack as shown in Fig.9(a), the values of λ can be obtained by solving the following eigenequations[3,26]:

$$\begin{aligned} D\,(\alpha,\beta,\lambda) = {} & \left[\cos^2\left(\frac{\pi}{2}\lambda\right) - (1-\lambda)^2\right]^2 \beta^2 + 2\,(1-\lambda)^2 \left[\cos^2\left(\frac{\pi}{2}\lambda\right) - (1-\lambda)^2\right] \alpha\beta \\ & + (1-\lambda)^2 \left[(1-\lambda)^2 - 1\right] \alpha^2 + \cos^2\left(\frac{\lambda\pi}{2}\right) \sin^2\left(\frac{\lambda\pi}{2}\right) = 0 \end{aligned} \tag{17}$$

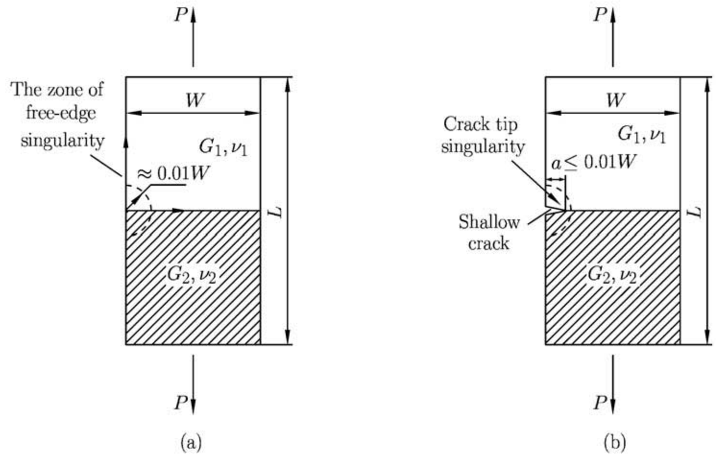

Fig. 9. (a) Free edge singularity of an un-cracked bonded strip and (b) crack tip singularity of a shallow edge interface crack in a dissimilar bonded strip.

where, when singularity exists near the interface corner, λ is the zero of $D(\alpha, \beta, \lambda)$ in $0 < \mathrm{Re}(\lambda) < 1$ that has the smallest real part. In general, $D(\alpha, \beta, \lambda)$ is expected to have several zeros in $0 < \mathrm{Re}(\lambda) < 1$. In all cases where more than one zero of $D(\alpha, \beta, \lambda)$ occurs only the smallest one will be exhibited[3]. The values of λ are computed for arbitrary material composite parameters (α, β) in the authors' previous research[17].

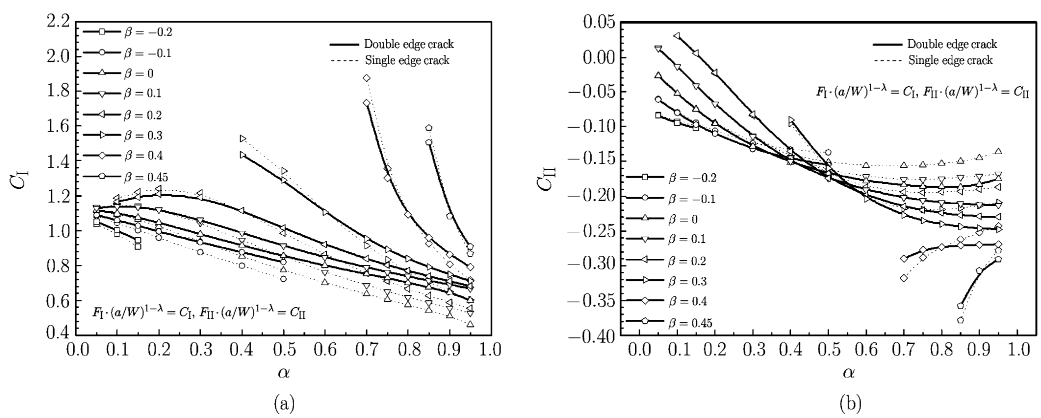

Fig. 10. Values of C_{I}, C_{II} of Eq.(16) for single and double edge interface cracks.

The constants C_{I}, C_{II} in Eq.(16) for the double edge crack case are computed for various material composite parameters. The values of C_{I}, C_{II} are plotted and tabulated against (α, β) in Figs.10(a) and (b) as well as in Table 4 and Table 5, respectively.

Recalling Eq.(16) and Fig.10, we know the stress intensity factors at the crack tip for the two types of cracks with the same relative crack length a/W within the singular zone of a bonded strip (shallow crack, $a/W < 0.01$) have the following relationships:

$F_{\mathrm{I,Dbl}} > F_{\mathrm{I,Sgl}}$, $F_{\mathrm{II,Dbl}} > F_{\mathrm{II,Sgl}}$, when $\alpha(\alpha - 2\beta) > 0$;

$F_{\mathrm{I,Dbl}} = F_{\mathrm{I,Sgl}}$, $F_{\mathrm{II,Dbl}} = F_{\mathrm{II,Sgl}}$, when $\alpha(\alpha - 2\beta) = 0$;

$F_{\mathrm{I,Dbl}} < F_{\mathrm{I,Sgl}}$, $F_{\mathrm{II,Dbl}} < F_{\mathrm{II,Sgl}}$, when $\alpha(\alpha - 2\beta) < 0$.

where, $F_{\mathrm{I,Dbl}}$, $F_{\mathrm{II,Dbl}}$ denote the normalized stress intensity factors within the singular zone for a double edge interface crack, and $F_{\mathrm{I,Sgl}}, F_{\mathrm{II,Sgl}}$ denote those for a single edge interface crack.

The size of the zone of dominance of free-edge singularity can be determined in a manner as given below. The double logarithmic lines for the single and double edge interface cracks under the same material parameters should be parallel (the line slopes are equal to the order of stress singularity $1-\lambda$).

Table 4. **Tabulated values of C_{I}**

α	$\beta=-0.2$	$\beta=-0.1$	$\beta=0$	$\beta=0.1$	$\beta=0.2$	$\beta=0.3$	$\beta=0.4$	$\beta=0.45$
0.05	1.05	1.089	1.116	1.131				
0.1	1.002	1.059	1.1	1.139	1.166			
0.15	0.945	1.027	1.076	1.135	1.193			
0.2		0.994	1.046	1.12	1.209			
0.3		0.932	0.98	1.061	1.191			
0.4		0.875	0.914	0.987	1.115	1.434		
0.5		0.819	0.854	0.913	1.015	1.29		
0.6			0.8	0.847	0.92	1.106		
0.7			0.75	0.789	0.838	0.954	1.734	
0.75			0.729	0.762	0.802	0.892	1.302	
0.8			0.7	0.737	0.769	0.838	1.092	
0.85			0.674	0.713	0.738	0.791	0.959	1.505
0.9			0.645	0.69	0.709	0.749	0.864	1.083
0.95			0.6	0.667	0.681	0.711	0.791	0.907

Table 5. **Tabulated values of C_{II}**

α	$\beta=-0.2$	$\beta=-0.1$	$\beta=0$	$\beta=0.1$	$\beta=0.2$	$\beta=0.3$	$\beta=0.4$	$\beta=0.45$
0.05	−0.084	−0.061	−0.027	0.013				
0.1	−0.095	−0.08	−0.052	−0.013	0.031			
0.15	−0.102	−0.097	−0.075	−0.041	0.006			
0.2		−0.11	−0.096	−0.067	−0.022			
0.3		−0.132	−0.128	−0.114	−0.082			
0.4		−0.146	−0.151	−0.15	−0.135	−0.09		
0.5		−0.155	−0.167	−0.174	−0.174	−0.16		
0.6			−0.178	−0.191	−0.199	−0.204		
0.7			−0.184	−0.202	−0.215	−0.227	−0.29	
0.75			−0.186	−0.206	−0.22	−0.235	−0.277	
0.8			−0.186	−0.209	−0.224	−0.24	−0.273	
0.85			−0.187	−0.211	−0.227	−0.244	−0.271	−0.358
0.9			−0.183	−0.212	−0.229	−0.246	−0.27	−0.307
0.95			−0.175	−0.213	−0.23	−0.248	−0.269	−0.291

Then, by examining the agreement of the slopes of the double logarithmic lines of F_{I}, F_{II} for the two cases with the theoretical values of $1-\lambda$ computed by Eq.(17) , the size of the singular zone can be determined. Take $\beta=0.3$ as an example. Extremely good agreement for the two slopes can be found for $a/W<0.001$ and an error within 5% for $a/W<0.01$. So, the size of the singular zone can be roughly decided as $a/W<0.01$. The singular zone along the interface in this paper almost agrees with that obtained by Reedy (1993) for an infinitely long biomaterial bonded strip under tension ($\alpha=-0.8$, $\beta=0$)[27]. More computations of the stress intensity factors for $0.001<a/W<0.01$ are needed to determine the size of the singular zone accurately.

3.3.2. Stress intensity factors for double edge interface cracks outside the zone of free-edge singularity

The normalized stress intensity factor curves of three typical material combinations shown in Fig.8 are chosen and plotted in Fig.11. As can be seen from the figure, the whole transverse region of the bonded strip shown in Fig.1(c) can be separated into three different zones. That is, they are denoted as zones 1, 2 and 3 as shown in Fig.11 for notational convenient. The boundaries of zones 1 and 2 as well as zones 2 and 3 are roughly defined as $0.01W$ and $0.1W$, respectively. Zone 1 is termed the zone of dominance of free-edge singularity, and has been discussed in §3.3.1. If the crack length is located in zone 1 ($a/W\le 0.01$), the stress intensity factors for the two types of cracks can be obtained by Eq.(16). Zone 2 is regarded as the transitional zone between zones 1 and 3. As can be seen from Fig.11, the stress intensity factors of a single edge interface crack within zone 3 are always bigger than those of a double edge interface crack. This phenomenon is caused by the counterbalance effect of the symmetry of the double edge interface crack. However, when the crack is located in zone 2 (say, $0.01\le a/W\le 0.1$), the relationships of the stress intensity factors for the two types of cracks become complex and have

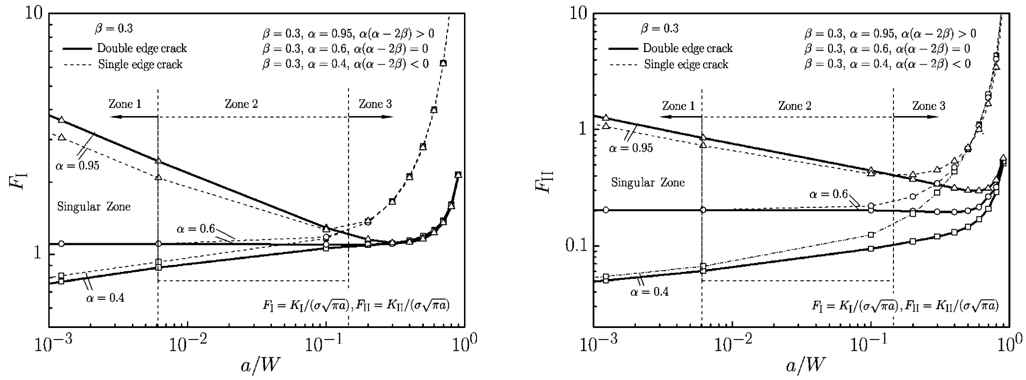

(a) (b)

Fig. 11. Three different zones for a dissimilar bonded strip.

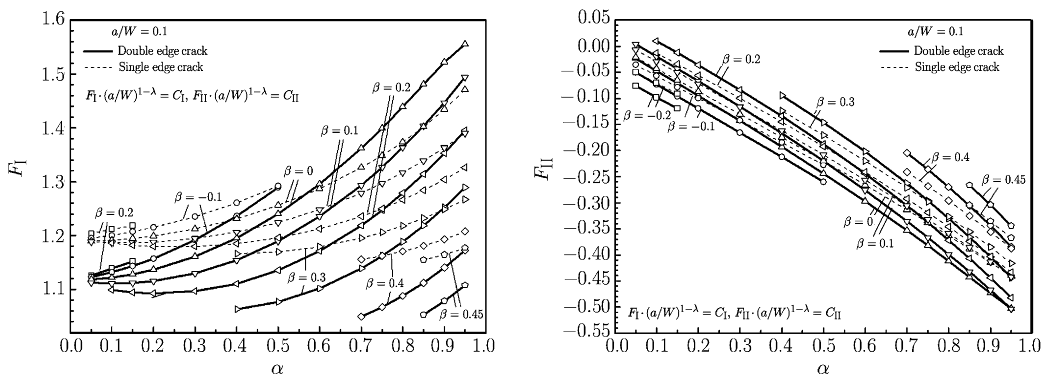

(a) (b)

Fig. 12. (a) $F_{\mathrm{I}} = K_{\mathrm{I}}/(\sigma\sqrt{\pi a})$ and (b) $F_{\mathrm{II}} = K_{\mathrm{II}}/(\sigma\sqrt{\pi a})$ for a single and a double edge interface crack ($a/W = 0.1$).

no unique or clear regular pattern to follow. In this case, the stress intensity factors are determined by the combined effect of the free-edge singularity and the symmetrical counterbalance. Generally, the left part of zone 2 is mainly affected by the free-edge singularity and the right part is dominated by the counterbalance effect. Specifically, F_{I}, F_{II} for $a/W = 0.1$ (zone 2) are plotted against different forms of combination of materials in Figs.12(a) and (b), respectively. It can be seen clearly that the stress intensity factors for a double edge interface crack can still be bigger than those of a single edge crack for specific forms of combination of materials. Figures 13(a) and (b) show the variation of F_{I}, F_{II} for $a/W = 0.2$ (zone 3) for different combination of materials, respectively. Figures 13(a) and (b) show that the absolute values of F_{I}, F_{II} for a single edge crack are always bigger than those of a double edge crack.

IV. CONCLUSIONS

The stress intensity factors can be evaluated by using the ratio of numerical solutions of the stress components computed by an ordinary numerical code (see FEM) for the reference and the target unknown problems. In this paper, variations of the normalized stress intensity factors F_{I}, F_{II} at the crack tip of the single and double edge interface cracks in a bi-material bonded strip were investigated and indicated for various forms of combination of materials and relative crack lengths a/W. Then, those for the two types of cracks were systematically compared. It was found in this research that the stress intensity factors for the double edge interface crack also exhibit a similar double logarithmic relationship as those of the single edge interface crack. Furthermore, the values of the double edge interface cracks can also be bigger than those of the single edge interface cracks.

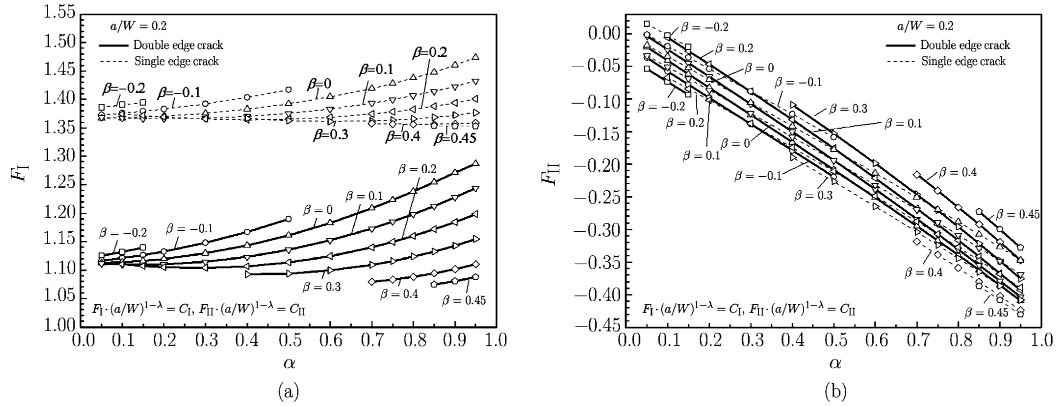

Fig. 13. (a) $F_{\mathrm{I}} = K_{\mathrm{I}}/(\sigma\sqrt{\pi a})$ and (b) $F_{\mathrm{II}} = K_{\mathrm{II}}/(\sigma\sqrt{\pi a})$ for a single and a double edge interface crack ($a/W = 0.2$).

References

[1] Williams,M.L., Stress singularities resulting from various boundary conditions in angular corners of plates in extension. *Journal of Applied Mechanics*, 1952, 19: 526-528.

[2] Hein,V.L. and Erdogan,F., Stress singularities in a two-material wedge. *International Journal of Fracture Mechanics*, 1971, 7: 317-330.

[3] Bogy,D.B. and Wang,K.C., Stress singularities at interface corners in bonded dissimilar isotropic elastic materials. *International Journal of Solids and Structures*, 1971, 7: 993-1005.

[4] Dempsey,J.P. and Sinclair G.B., On the stress singularities in the plane elasticity of the composite wedge. *Journal of Elasticity*, 1979, 9: 373-391.

[5] Van Vroonhoven,J.C.W., Stress singularities in bi-material wedges with adhesion and delamination. *Fatigue and Fracture Engineering Materials and Structures*, 1992, 15: 157-171.

[6] Bogy,D.B., Two edge-bonded elastic wedges of different materials and wedges angles under surface tractions. *Journal of Applied Mechanics*, 1971, 38: 377-386.

[7] Vasilopoulos,D., On the determination of higher-order terms of singular elastic stress fields near corners. *Numerical Mathematics*, 1988, 53: 51-59.

[8] Theocaris,P.S., The order of singularity at a multi-wedge corner in a composite plate. *International Journal of Engineering Science*, 1974, 12: 107-120.

[9] Dempsey,J.P. and Sinclair,G.B., On the singular behavior at the vertex of a bi-material wedge, *Journal of Elasticity*, 1981, 11: 317-327.

[10] Wu,Y.L., A new method for evaluation of stress intensities for interface cracks. *Engineering Fracture Mechanics*, 1994, 48: 755-761.

[11] Yang,X.X. and Kuang,Z.B., Contour integral method for stress intensity factors of interface crack. *International Journal of Fracture*, 1996, 78: 299-313.

[12] Munz,D. and Yang,Y.Y., Stress singularities at the interface in bonded dissimilar materials under mechanical and thermal loading. *Journal of Applied Mechanics*, 1992, 59: 857-861.

[13] Dong,Y.X., Wang,Z.M. and Wang,B., On the computation of stress intensity factors for interfacial cracks using quarter point boundary elements. *Engineering Fracture Mechanics*, 1997, 57: 335-342.

[14] Liu,Y.H., WU,Z.G., Liang Y.C. and Liu,X.M., Numerical methods for determination of stress intensity factors of singular stress field. *Engineering Fracture Mechanics*, 2008, 75: 4793-4803.

[15] Oda,K., Kamisugi,K. and Noda,N.A., Analysis of stress intensity factor for interface cracks based on proportional method. *Transactions of Japan Society of Mechanical Engineers, Series A*, 2009, 75: 476-482.

[16] Teranishi,T. and Nisitani,H., Determination of highly accurate values of stress intensity factor in a plate of arbitrary form by FEM. *Transactions of Japan Society of Mechanical Engineers, Series A*, 1999, 65(635): 16-21.

[17] Noda,N.A., Lan,X., Michinaka,K., Zhang,Y. and Oda,K., Stress intensity factor of an edge interface crack in a bonded semi-infinite plate. *Transactions of Japan Society of Mechanical Engineers, Series A*, 2010, 76(770): 1270-1277.

[18] Lan,X., Noda,N.A., Michinaka,K. and Zhang,Y., The effect of material combinations and relative crack size to the stress intensity factors at the crack tip of a bi-material bonded strip. *Engineering Fracture Mechanics*, 2011, 78: 2572-2584.

[19] Erdogan,F., Stress distribution in bonded dissimilar materials with cracks. *Transactions of ASME, Journal of Applied Mechanics*, 1965, 32: 403-410.

[20] Kaya,A.C. and Erdogan,F., On the solution of integral equations with strongly singular kernels. *Quarter of Applied Mathematics*, 1987, 45(1): 105-122.

[21] Noda,N.A., Araki,K. and Erdogan,F., Stress intensity factors in two bonded elastic layers with a single edge crack under various loading conditions. *International Journal of Fracture*, 1992, 57: 101-126.

[22] Nisitani,H, Chen,D.H. and Samimoto,A., Versatile Program of Two-Dimensional Stress Analysis Based on Body Fore Method. Tyoko: Baifukan, 1994 (in Japanese).

[23] Matsumto,T., Masataka,T. and Obara,R., Computation of stress intensity factors of interface cracks based on interaction energy release rates and BEM sensitivity analysis. *Engineering Fracture Mechanics*, 2000, 65: 683-702.

[24] Yuuki,R. and Cho,S.B., Efficient boundary element analysis of stress intensity factors for interface cracks in dissimilar materials. *Engineering Fracture Mechanics*, 1989, 34: 179-188.

[25] Ikeda,N., Soda,T. and Munakata,T., Stress intensity factor analysis of interface crack using boundary element method—Application of contour-integral method. *Engineering Fracture Mechanics*, 1993, 45: 599-610.

[26] Chen,D.H. and Nishitani,H., Intensity of singular stress field near the interface edge point of a bonded strip. *Transactions of Japan Society of Mechanical Engineers, Series A*, 1993, 59: 2682-2686.

[27] Reedy,Jr., Asymptotic interface-corner solutions for butt tensile joints. *International Journal of Solids and Structures*, 1993, 30: 767-777.